Fish and Shellfish Immunology 87 (2019) 32–42

Contents lists available at ScienceDirect

Fish and Shellfish Immunology

journal homepage: www.elsevier.com/locate/fsi

Short communication

Two phospholipid scramblase 1–related proteins (PLSCR1like-a & -b) from *Liza haematocheila:* Molecular and transcriptional features and expression analysis after immune stimulation

W.M. Gayashani Sandamalika[a], Thanthrige Thiunuwan Priyathilaka[a], Bo-Hye Nam[b], Jehee Lee[a,*]

[a] Department of Marine Life Sciences & Fish Vaccine Research Center, Jeju National University, Jeju Self-Governing Province, 63243, Republic of Korea
[b] Biotechnology Research Division, National Institute of Fisheries Science, 408-1 Sirang-ri, Gijang-up, Gijang-gun, Busan, 46083, Republic of Korea

ARTICLE INFO

Keywords:
Phospholipid scramblase 1 like
PLSCR
Red lip mullet
Liza haematocheila
Immune response

ABSTRACT

Phospholipid scramblases (PLSCRs) are a family of transmembrane proteins known to be responsible for Ca^{2+}-mediated bidirectional phospholipid translocation in the plasma membrane. Apart from the scrambling activity of PLSCRs, recent studies revealed their diverse other roles, including antiviral defense, tumorigenesis, protein–DNA interactions, apoptosis regulation, and cell activation. Nonetheless, the biological and transcriptional functions of PLSCRs in fish have not been discovered to date. Therefore, in this study, two new members related to the PLSCR1 family were identified in the red lip mullet (*Liza haematocheila*) as *MuPLSCR1like-a* and *MuPLSCR1like-b*, and their characteristics were studied at molecular and transcriptional levels. Sequence analysis revealed that MuPLSCR1like-a and MuPLSCR1like-b are composed of 245 and 228 amino acid residues (aa) with the predicted molecular weights of 27.82 and 25.74 kDa, respectively. A constructed phylogenetic tree showed that MuPLSCR1like-a and MuPLSCR1like-b are clustered together with other known PLSCR1 and -2 orthologues, thus pointing to the relatedness to both PLSCR1 and PLSCR2 families. Two-dimensional (2D) and 3D graphical representations illustrated the well-known 12-stranded β-barrel structure of MuPLSCR1like-a and MuPLSCR1like-b with transmembrane orientation toward the phospholipid bilayer. In analysis of tissue-specific expression, the highest expression of *MuPLSCR1like-a* was observed in the intestine, whereas *MuPLSCR1like-b* was highly expressed in the brain, indicating isoform specificity. Of note, we found that the transcription of *MuPLSCR1like-a* and *MuPLSCR1like-b* was significantly upregulated when the fish were stimulated with poly (I:C), suggesting that such immune responses target viral infections. Overall, this study provides the first experimental insight into the characteristics and immune-system relevance of *PLSCR1*-related genes in red lip mullets.

1. Introduction

In all living organisms, cellular membranes consist of a double layer of lipids known as phospholipids where proteins are embedded [1]. In the plasma membrane, out of a variety of phospholipids, phosphatidylcholine (PC) and sphingomyelin (SM) are located in the extracellular leaflet, while phosphatidylethanolamine (PE) and phosphatidylserine (PS) are present only in the cytoplasmic leaflet [2]. Under normal conditions, cells maintain this membrane asymmetry, and it gets disrupted under some critical conditions, such as activation of cells, coagulation, and apoptosis, which may be affected by the phospholipid translocation [3].

Amino phospholipid translocases are the enzymes that can move PS to the cell surface from the inner leaflet by means of passive diffusion [4,5]. Nonetheless, when considering the time required for the overall process of apoptotic cell death culminating cell lysis, it takes a similar amount of time or less than that of the halftime for trans-bilayer diffusion [4]. Therefore, it is clear that another membrane protein is involved in the above process for the rapid movement of PS to the cell surface and effective removal of apoptotic cells before the initiation of cell lysis and inflammation [4]. This protein has been identified as phospholipid scramblase (PLSCR), a nonspecific lipid flippase, which allows for rapid flipping through lipid bilayers and effectively disturbs the asymmetry of phospholipid bilayers [6]. Aside from apoptotic cells, this mechanism can also be observed in platelets, which eventually activate the process of blood coagulation [7].

* Corresponding author. Marine Molecular Genetics Lab, Department of Marine Life Sciences, Jeju National University, Jeju Self-Governing Province, 63243, Republic of Korea.
E-mail address: jehee@jejunu.ac.kr (J. Lee).

https://doi.org/10.1016/j.fsi.2018.12.044
Received 23 June 2018; Received in revised form 17 December 2018; Accepted 21 December 2018
Available online 26 December 2018
1050-4648/

It has been reported that the recognition of cell membrane surface PS and limiting the PS localization to the outer leaflet of the plasma membrane have been phylogenetically conserved in vertebrates and mammals for millions of years [8]. However the identity and the mechanisms of their regulation for control over PS distribution are not clarified well [6]. On the other hand, scramblases get activated in response to an increment of Ca^{2+} concentration, and after activation they get redistributed throughout the plasma membrane rapidly via an unknown mechanism. As a result of this change, the targeted cellular membrane PL bilayer loses its asymmetry [6].

PLSCRs consist of several functionally important domains. They are named as proline-rich N-terminal domain, cysteine-rich region, the Ca^{2+}-binding motif, a nuclear localization signal (NLS), the DNA-binding motif, and a transmembrane region [3,9]. All these identified domains have specific functions. The N-terminal region contains multiple proline-rich domains, which interact with SH3 and WW domain–containing proteins [10]. The Ca^{2+}-binding motif is required for Ca^{2+}-binding and activation [11], whereas the cysteine-rich motif is involved in membrane anchoring [12]. The DNA-binding motif is responsible for the protein–DNA interactions in transcriptional regulation [3]. A nonclassical NLS is essential for the nuclear localization of PLSCRs [9], and the transmembrane region is required for insertion into the membrane [3].

PLSCRs are a group of homologous proteins, and four isoforms have been identified in humans named as hPLSCR1–hPLSCR4 [13]. The functions of hPLSCR1 have been identified as expression of different levels of PS on the cell surface, regulation of blood coagulation properties, and effective contribution to apoptosis [11]. Besides, recent studies revealed that hPLSCR1 interacts with cell signaling pathways and works as a transcription factor in activation of other genes [3,14]. Although hPLSCR1, -3, and -4 are detectable in various types of tissues, there are a few exceptions [3]. hPLSCR1 and -3 are undetectable in the brain, whereas hPLSCR4 is absent in peripheral-blood lymphocytes [3]. Moreover, hPLSCR2 is restricted to testes [3]. hPLSCRs have been documented as multifunctional proteins because they are involved in the main cellular processes like cell proliferation [15], antiviral responses [16–18], apoptosis [8,18,19], transcriptional regulation [18], tumor suppression, and protein interactions. Most of the documented experiments with PLSCRs are carried out to identify the roles of human PLSCRs. Recently, aside from human studies, some reports on PLSCRs of planarian *Dugesia japonica* [20], mice, and *Drosophila melanogaster* became available [21]. Moreover, a study focused on PLSCRs of *D. japonica* have explained the involvement of PLSCRs in immune responses upon pathogen invasion [20]. To date, no records are available for any study on PLSCRs in fish. Therefore, this report is the first attempt at characterization of PLSCR1 from fish, with a focus on its molecular mechanism of action and immunological functions.

Red lip mullets (*Liza haematocheila*) are naturally populated in tropical and temperate regions of the world, and are considered an important aquaculture species in Korea, Japan, Taiwan, China, and in the North West Pacific Ocean [22,23]. Recently, mass mortality of red lip mullets was observed during cultivation, and a gram-positive bacterium, *Lactococcus garvieae* was identified as a causative agent of green liver syndrome in red lip mullets [22]. It has caused outbreaks of the disease and mass mortality of mullets in several countries, including Korea [22]. Therefore, identification of novel immunity-related genes as well as their responses to pathogens is essential for disease prevention and development of the aquaculture industry. In this study, two *PLSCR1*-related genes: *PLSCR1like-a* and *PLSCR1like-b* were identified in the red lip mullet and molecularly characterized [3]. Furthermore, their involvement in post-immune responses to live bacteria and potent immune stimulants were determined.

2. Materials and methods

2.1. Experimental fish rearing and tissue collection

Red lip mullets were purchased from the Sangdeok fishery in Hadong, Korea. The average body weight of selected fish was set to be as 100 g. They were acclimated to the laboratory conditions, by rearing in 40 L flat-bottomed tanks with aerated and sand-filtered sea water for 7 days prior to the experiment. Salinity and temperature were maintained at 34 ± 0.6‰ and 20 ± 1 °C, respectively.

For tissue-specific expression analysis, five mullets were selected with the 100 g average body weight and were anesthetized conventionally (MS-222; 40 mg/L). For blood collection, heparin sodium salt (USB, USA)-coated sterile syringes were used to withdraw whole blood from the caudal vein of a mullet (~1 mL/fish), and the peripheral blood cells were separated immediately by the means of centrifugation at 3000 × *g* for 10 min at 4 °C. After collection of blood, 11 types of tissues were collected including the head kidney, spleen, liver, muscle, gills, intestine, kidneys, brain, skin, heart, and stomach by dissection. All the collected tissues were immediately snap-frozen in liquid nitrogen and stored at −80 °C.

Another set of mullets was divided into four groups with 100 g average body weight and was subjected to an immune challenge experiment. Lipopolysaccharide (LPS; 1.25 μg/g, from *Escherichia coli* 055:B5; Sigma, St. Louis, MO, USA), polyinosinic:polycytidylic acid [poly(I:C) 1.5 μg/g], and *Lactococcus garvieae* (1×10^3 colony-forming units [CFU]/μL), were prepared in phosphate-buffered saline (PBS), and 100 μL was injected intraperitoneally into the fish. The control group of fish was injected with 100 μL of PBS. After the challenge, tissues from the spleen & head kidney were collected from five individuals at 0, 6, 24, 48, or 72 h postinjection (p.i.) by the same method as described above. All the collected samples were snap-frozen and stored at −80 °C until used for RNA extraction.

2.2. RNA extraction and cDNA synthesis

For tissue distribution and immune-challenge experiments, the collected tissue samples were pooled (n = 5), and total RNA was extracted by means of RNAiso plus (TaKaRa, Japan) followed by clean-up on RNeasy Spin Columns (Qiagen). The quality of RNA was determined by running 1.5% agarose gel electrophoresis and the concentration at 260 nm was measured using μDrop Plate (Thermo Scientific). The first-strand cDNA was synthesized with the Prime Script™ II 1st strand cDNA Synthesis Kit (Takara, Japan). The total volume of 20 μL reaction mixture was prepared which contained 2.5 μg of total RNA. Synthesized cDNA was diluted 40-fold with nuclease-free water and stored at −80 °C until further use.

2.3. Identification and sequence analysis of MuPLSCR1like proteins

A cDNA database of the red lip mullet was established via the PacBio sequencing technology [24]. The Basic Local Alignment Search Tool (BLAST) [25], at the National Center for Biotechnology Information (NCBI) web-based query system (http://www.ncbi.nlm.nih.gov/BLAST), was used to identify putative *MuPLSCR1like-a & -b*. The complete open reading frames (ORFs) and their corresponding amino acid sequences were determined by means of an online server, ORF finder (https://www.ncbi.nlm.nih.gov/orffinder/). The SignalP software was used (http://www.cbs.dtu.dk/services/SignalP) to determine the availability and the localization of signal peptides [26], while predicting the protein domains and functional sites by analysis in ExPASy prosite (http://prosite.expasy.org) [27]. The Molecular Evolutionary Genetics Analysis (MEGA) version 6.0 software served for comparative analysis of evolutionary relations by constructing the phylogenetic tree via the Neighbor-joining method with 1000 bootstrap replicates [28]. Pairwise sequence alignment was performed with the EMBOSS Needle

Table 1
Sequences of primers used in this study.

Primer name	Application	Sequence of primer (5′-3′)
MuPLSCR1like-a _qF	qPCR amplification	GTGAGGTCTCTGGATGAGTCGATGG
MuPLSCR1like-a _qR		TCCCACCATCACAGCCTTCAT
MuPLSCR1like-b _qF		GCGTAACTCCATGGGCCAGAAC
MuPLSCR1like-b _qR		AGTGGTCTGGTGACGCTGATG
MuEF1α F	qPCR Internal reference	CCCTGGTCAGATCAGTGCTGGTTAT
MuEF1α R		AGCGTCGCCAGACTTTAGGGATTT

(https://www.ebi.ac.uk/Tools/services/web/toolresult.ebi) web-based tool [29]. Multiple sequence alignment was generated by Clustal omega (http://www.ebi.ac.uk/Tools/msa/clustalo) [30] and Color align conservation (http://www.bioinformatics.org/sms2/color_align_cons.html) [31] web-based tool using the amino acid sequences obtained from the BLAST analysis. 2D structure was modeled on the PRED-TMBB (http://bioinformatics.biol.uoa.gr/PRED-TMBB/) web server [32]. To reveal 3D structure of MuPLSCR1like-a & -b, Swiss model (https://swissmodel.expasy.org) protein structure homology-modeling server [33] was used, and the results were visualized in PyMOL v.1.5 software [34].

2.4. Transcriptional analysis by quantitative real time PCR (qPCR)

Transcriptional analysis in groups of unchallenged and immune challenged mullets was performed by qPCR on a Thermal Cycler Dice™ TP950 (Takara, Japan) following manufacturer's instructions. SYBR Green served as the fluorescent agent. For amplification of genes, gene-specific primers were designed according to the MIQE guidelines [35] (Table 1). The total reaction mixture was 10 μL and consisted of 3 μL of a diluted cDNA template, 5 μL of 2× TaKaRa ExTaq™ SYBR premix, 0.4 μL of each forward and reverse primer (10 pmol/μL), and 1.2 μL of dH_2O (PCR grade). The qRT-PCR cycling program included a single cycle of 95 °C for 10 s; followed by 45 cycles of 95 °C for 5 s, 58 °C for 10 s, and 72 °C for 20 s; and a final single cycle of 95 °C for 15 s, 60 °C for 30 s, and 95 °C for 15 s. All analyses were performed in triplicate to increase accuracy. For the standardization, mullet elongation factor 1 alpha (EF1α) (accession No.: MH017208) served as the internal control gene in the analysis with corresponding primers. By the Livak ($2^{-\Delta\Delta CT}$) method [36] the relative mRNA expression levels were analyzed quantitatively. All the data from challenged groups were normalized to the relevant PBS control at each time point. All the obtained data were presented as fold changes (means ± standard deviation [SD]) using the 0 h expression of un-injected control as the basal level reference. To evaluate the statistical significance of the data, they were subjected to statistical analysis in the SPSS 16.0 software (USA). One-way analysis of variance (ANOVA) followed by Duncan's *post hoc* comparison test was carried out for the analysis of tissue-specific mRNA expression levels. The unpaired Student's *t*-test was conducted in the immune challenge experiment for analyzing the significance of differences between control and experimental groups. Statistically significant data were obtained by considering the *P* values, less than 0.05 ($P < 0.05$).

3. Results

3.1. Identification and characterization of MuPLSCR1like-a and b

Two cDNA contigs belonging to the PLSCR family were identified in the red lip mullet transcriptome database using BLAST analysis and were designated as *MuPLSCR1like-a and MuPLSCR1like-b*.

The *MuPLSCR1like-a* (GenBank accession No: MH511809) encodes a polypeptide of 245 aa with a predicted 27.82 kDa molecular weight. The theoretical isoelectric point (pI) and the instability index of MuPLSCR1like-a were found to be 4.79 and 53.59, respectively. *MuPLSCR1like-b* (GenBank accession No: MH511810) encodes a polypeptide of 228 aa with predicted 25.74 kDa molecular weight. *MuPLSCR1like-b* has a theoretical pI value of 4.75. The instability index for *MuPLSCR1like-b* was calculated too: 49.51.

To identify the different characteristics of MuPLSCR1like-a and -b, analyses of several domains and motifs were performed. The protein sequence analysis performed by SignalP 4.1 server revealed that both MuPLSCR1like-a and MuPLSCR1like-b do not contain any signal peptides. Remarkably, in MuPLSCR1like-a, a DNA-binding motif was identified at positions 18–51 (aa), and a cysteine-rich region was identified at aa positions 113–121. MuPLSCR1like-a contained the NLS domain at aa positions 188–198 and a Ca^{2+}-binding motif was detected in the region 203–216 aa. Furthermore, a transmembrane region was detected at the C terminus at aa positions 220–238 in MuPLSCR1like-a. By contrast, in MuPLSCR1like-a, no proline-rich N-terminal domain could be detected by the protein sequence analysis. Similarly, MuPLSCR1like-b contains a DNA-binding motif at aa positions 5–37, an NLS domain at 175–186, and a Ca^{2+}-binding motif in the region 190–203 aa. The transmembrane region was detected at aa positions 207–225 in MuPLSCR1like-b. Nonetheless, no proline-rich N-terminal domain or cysteine-rich region were detected in MuPLSCR1like-b. Moreover, both MuPLSCR1like proteins have a final short exoplasmic tail at their C terminus. In MuPLSCR1like-a, the exoplasmic tail extends up to 7 aa (^{239}IKPQRDS^{245}), and in MuPLSCR1like1-b, it is only 3 aa long (^{226}ITN^{228}; Fig. 1).

3.2. Homology analysis of MuPLSCR1like-a and -b

Protein BLAST analysis suggested that MuPLSCR1like-a and -b were similar to other (previously described) PLSCR1 and PLSCR1like homologues. The identity and similarity percentages were determined using the pairwise sequence alignment (Table 2). The results indicated that the highest identity (I%) and similarity (S%) for both MuPLSCR1like-a (I-53.5%, S-66.9%) and MuPLSCR1like-b (I-96.9%, S-98.2%) were shared with PLSCR1like of a fish, *Fundulus heteroclitus*. Moreover, the data revealed that both MuPLSCR1like-a and -b share greater than 48% identity with other fish homologues (Table 2). The amino acid sequences of MuPLSCR1like-a and -b were compared with other orthologs from different taxonomic groups, and it was revealed that MuPLSCR1like-a and -b contain a conserved DNA-binding motif, a Ca^{2+}-binding motif, an NLS, and a C-terminal transmembrane region in their structure (Fig. 1). Only MuPLSCR1like-a has a conserved cysteine-rich region as identified by the sequence analysis. Nonetheless, both MuPLSCR1like-a and -b do not contain N-terminal proline-rich domains in their structures (Fig. 1).

3.3. The 2D and 3D structural analysis of MuPLSCR1like-a & -b

The 3D structures of both MuPLSCR1like proteins showed a 12-stranded symmetrical β-barrel, which encloses a central C-terminal α-helix (Fig. 2). The C-terminal helix is shown in side-to-outside orientation from the hollow cylinder. Based on the Posterior decoding algorithm in PRED-TMBB, topology of the protein structures was clearly determined with respect to the phospholipid bilayer (Fig. 3).

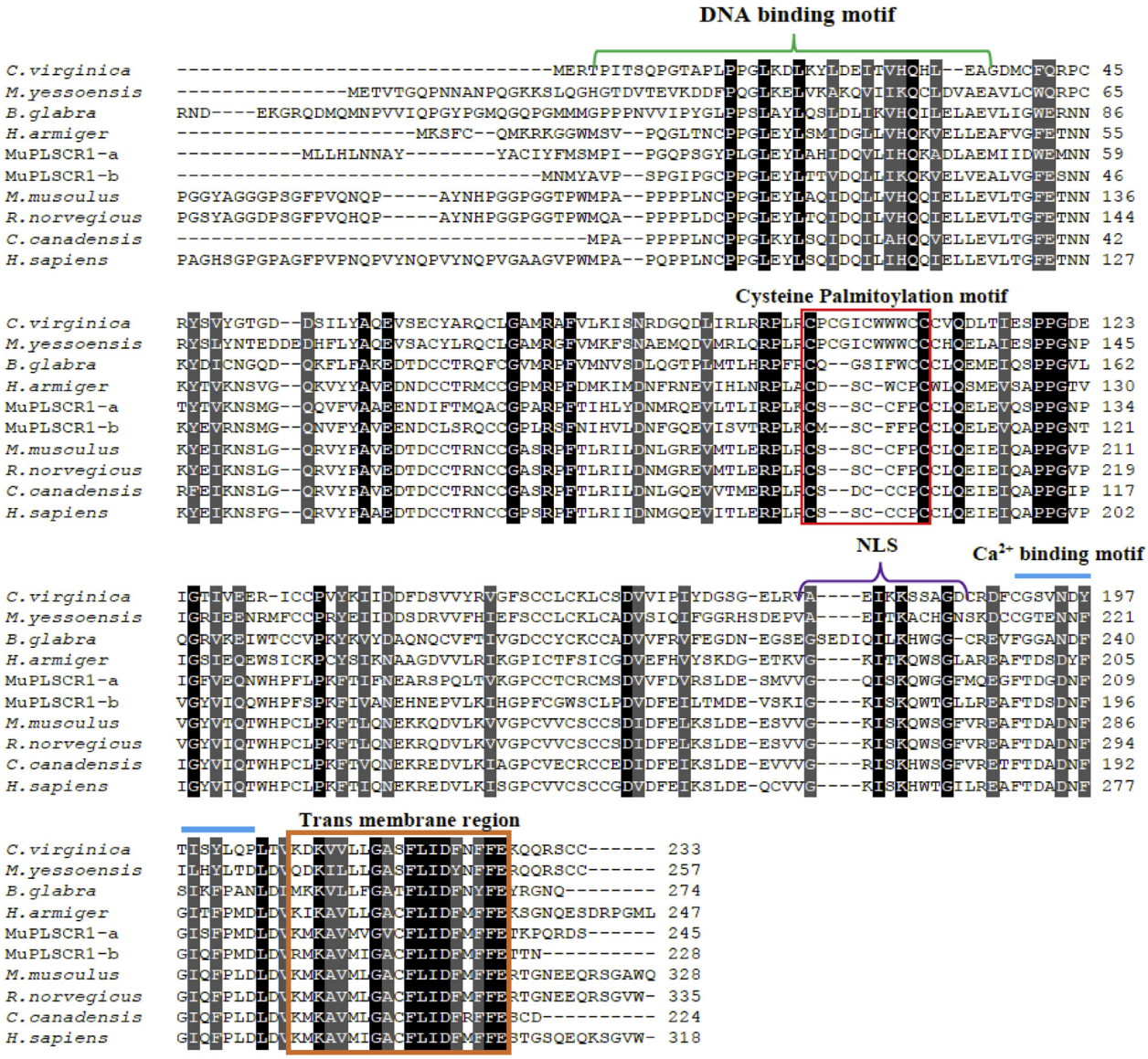

Fig. 1. Multiple-sequence alignment of the amino acid sequences of MuPLSCR1like-a & -b and its orthologs from different species. Fully conserved amino acids are shown in black, and strongly conserved and weakly conserved amino acids are highlighted in dark grey and light grey, respectively.

Table 2
Pairwise identity (I%), similarity (S%), and gaps (G%) of red lip mullet PLSCR1like proteins toward selected orthologs at amino acid levels.

Gene	Species	Accession no.	*MuPLSCR1like-a*			*MuPLSCR1like-b*			Taxonomy
			I (%)	S (%)	G (%)	I (%)	S (%)	G (%)	
MuPLSCR1like-a	Liza hematochelia	MH511809	100%	100%	0.0	54.7%	67.3%	6.9%	Fish
MuPLSCR1like-b	*Liza hematochelia*	MH511810	54.7%	67.3%	6.9%	100%	100%	0.0	Fish
PLSCR2	*Larimichthys Crocea*	KKF30002.1	54.7%	67.3%	6.9%	96.5%	98.7%	0.0	Fish
PLSCR1 Like	*Fundulus heteroclitus*	XP_012708587.1	53.5%	66.9%	6.9%	96.9%	98.2%	0.0%	Fish
PLSCR1 Like	*Danio rerio*	XP_693207.5	51.6%	63.4%	12.9%	52.7%	66.4%	17.7%	Fish
PLSCR1 Like	*Oncorhynchus mykiss*	XP_021420053.1	48.2%	61.8%	9.2%	53.8%	70.4%	7.5%	Fish
PLSCR1 Like	*Cyanistes caeruleus*	XP_023788895.1	46.2%	56.8%	24.3%	47.5%	60.9%	19.7%	Aves
PLSCR1 Like	*Lonchura striata domestica*	XP_021392490.1	44.9%	55.1%	24.6%	48.8%	60.4%	19.4%	Aves
PLSCR1 Like	*Rattus norvegicus*	XP_017451607.1	47.2%	63.6%	8.8%	51.5%	71.1%	7.1%	Mammal
hPLSCR1	*Homo sapiens*	NP_066928.1	44.0%	54.7%	23.0%	45.6%	56.3%	28.3%	Mammal
PLSCR1 Like	*Macaca nemestrina*	XP_011720023.1	42.1%	61.9%	6.5%	47.4%	67.9%	3.0%	Mammal
PLSCR1 Like	*Bos indicus*	XP_019816762.1	37.3%	56.8%	14.0%	39.8%	57.2%	15.5%	Mammal
PLSCR1 Like	*Xenopus laevis*	XP_018121282.1	39.2%	50.9%	31.3%	45.1%	57.6%	25.1%	Amphibia
PLSCR1 Like	*Mizuhopecten yessoensis*	XP_021374068.1	39.2%	50.7%	22.3%	44.1%	58.4%	18.9%	Mollusk
PLSCR1 Like	*Crassostrea virginica*	XP_022345293.1	21.5%	35.2%	24.4%	24.0%	38.3%	26.0%	Mollusk
PLSCR1 Like	*Limulus polyphemus*	XP_022256660.1	37.7%	48.9%	27.5%	47.1%	59.6%	23.9%	Arthropoda

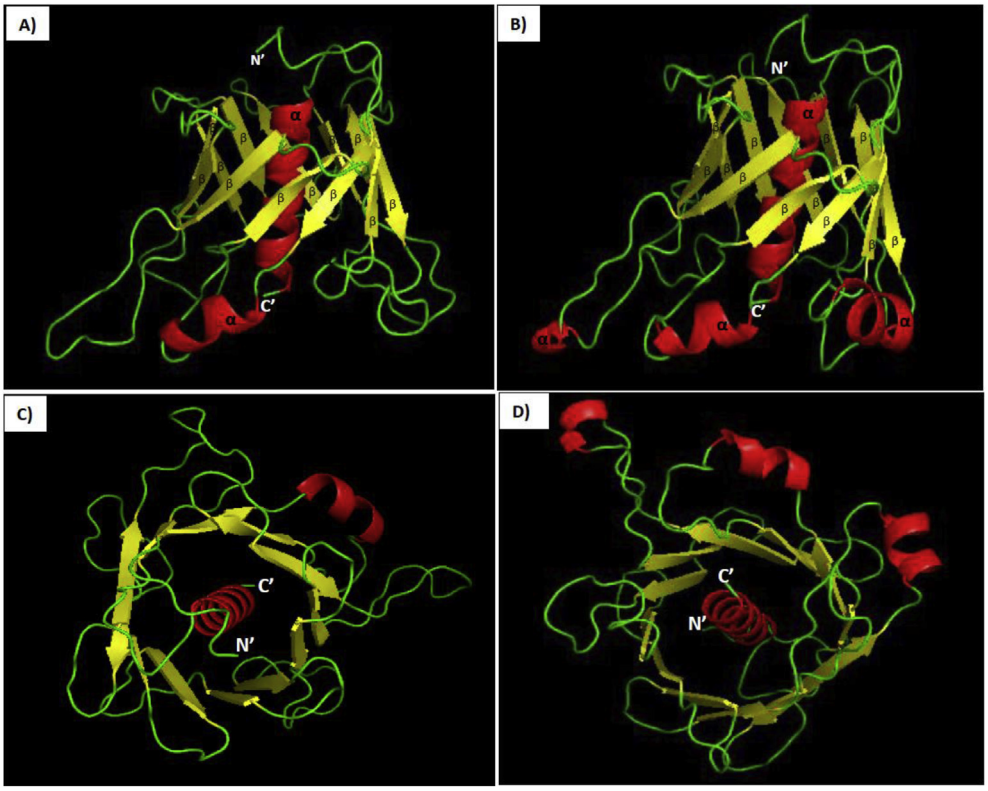

Fig. 2. A & B) Predicted 3D structures of MuPLSCR1like-a & -b, respectively. The α-helices and β-sheets are marked with the corresponding letters. **C & D)** The 12-stranded symmetrical β-barrel which encloses a central C-terminal α-helix in MuPLSCR1like-a & -b, respectively. The models of 3D structure were predicted using the Swiss-model server and were visualized in the PyMOL software.

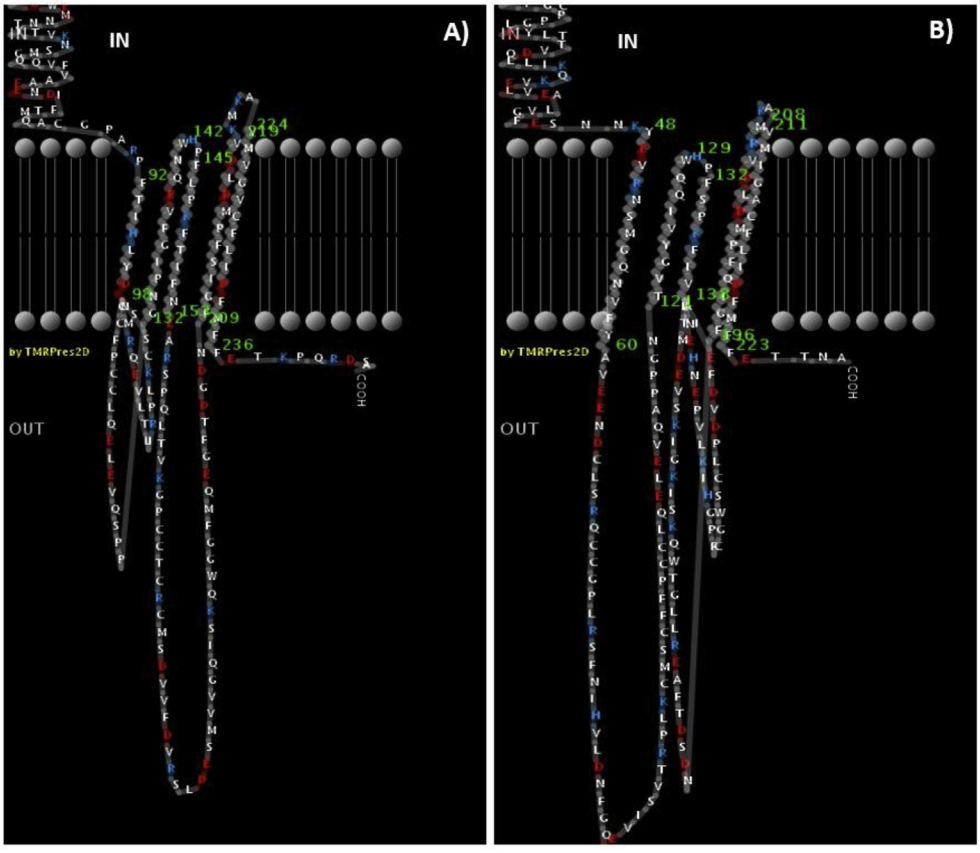

Fig. 3. A & B) Graphical representation of the predicted topology of MuPLSCR1like-a & -b with respect to the lipid bilayer. Output of the prediction obtained in the PRED-TMBB software by the posterior decoding method.

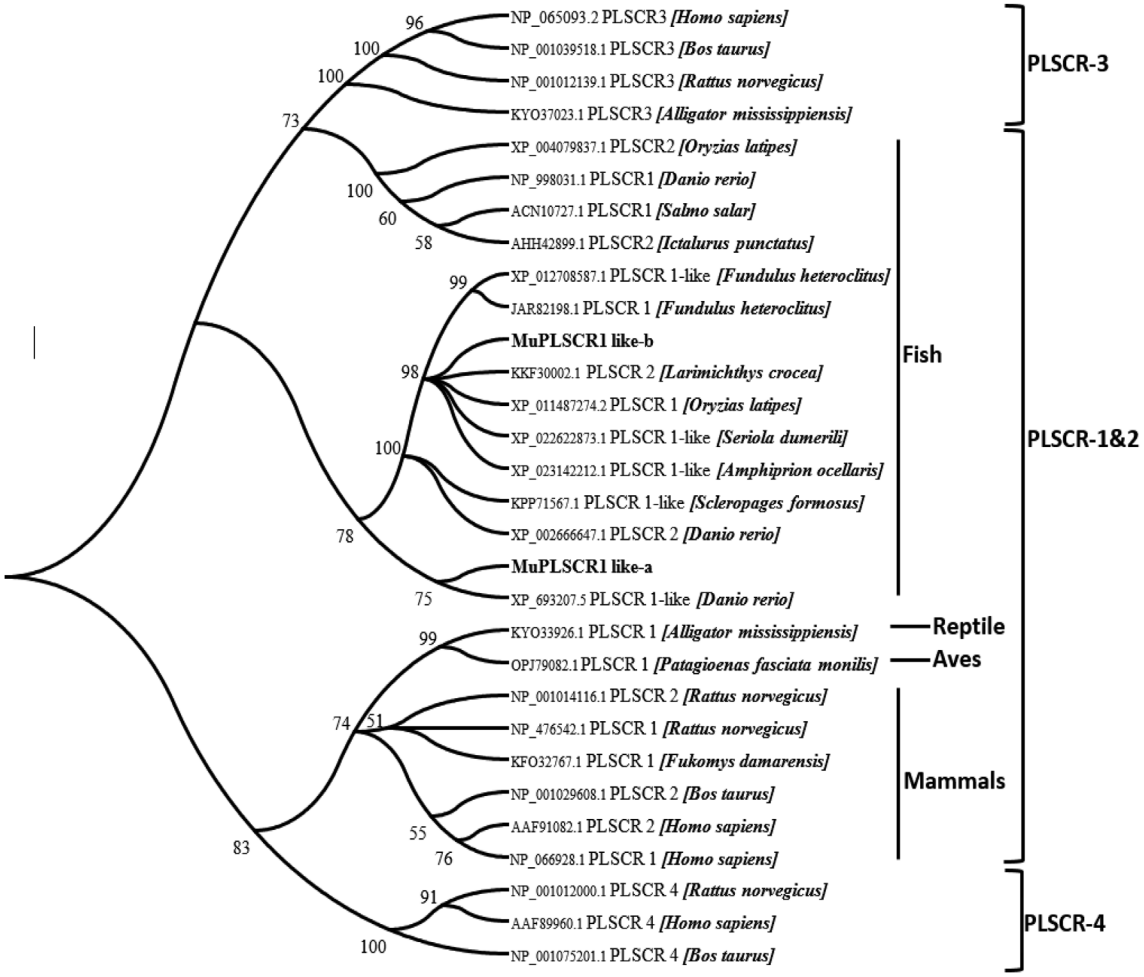

Fig. 4. A phylogenetic tree constructed by the neighbor-joining method based on different classes of PLSCRs. The bootstrap values are shown at the node of each branch. The NCBI accession numbers are given with each organism name.

3.4. Construction of the phylogenetic tree

The phylogenetic tree was constructed by the neighbor-joining method to evaluate the evolutionary relations among MuPLSCR1like proteins (Fig. 4.). According to these data, MuPLSCR1like-a and MuPLSCR1like-b are clustered in the same clade but from different branches together with other fishes' PLSCR1, PLSCR2, and PLSCR1like homologues. MuPLSCR1like-a showed close relatedness to PLSCR1like from *Danio rerio*. Additionally, MuPLSCR1like-b manifested a close relationship with PLSCR2 from *Larimichthys crocea* including PLSCR1 and PLSCR1like from other fish species.

3.5. Tissue distribution analysis of MuPLSCR1like-a and -b

Both *MuPLSCR1like-a* and *-b* were found to be expressed in all the examined tissues, including the head kidney, spleen, liver, gills, intestine, kidneys, brain, muscle, skin, heart, stomach, and blood, at different mRNA levels. *MuPLSCR1like-a* showed its highest expression in the intestine with ~56-fold value, following skin and muscle with ~43- and ~37-fold values, respectively ($p < 0.05$). In contrast, *MuPLSCR1like-b* manifested its strongest expression in the brain with a ~182-fold value, followed by muscle with a ~73-fold value ($p < 0.05$).

3.6. Expression analysis of MuPLSCR1like proteins after immune stimulation

To determine the potential involvement of *MuPLSCR1like-a* and *-b* in immune responses, transcriptional regulation in the spleen (Fig. 6 A–F) and the head kidney (Fig. 7 A–F) was analyzed at different time points, after injection of the fish with various immune stimulants including LPS, poly(I:C), or *Lactococus garvieae*. In the spleen, after stimulation with poly(I:C), the expression of *MuPLSCR1like-a* and *MuPLSCR1like-b* was significantly upregulated at 6 h p.i. (Fig. 6 A&D). The LPS treatment did not cause any significant upregulation or downregulation pattern for *MuPLSCR1like-a* as compared to the unchallenged group. Nevertheless, mRNA expression of *MuPLSCR1like-b* was significantly upregulated after 48 h p.i. (Fig. 6E). As for *MuPLSCR1like-a*, the treatment with *L. garvieae* did not significantly alter gene expression either. By contrast, regarding *MuPLSCR1like-b*, the *L. garvieae* treatment significantly upregulated the mRNA expression levels at 24 h p.i. (Fig. 6F).

In the head kidney, after poly(I:C) administration, only *MuPLSCR1like-a* was significantly upregulated at 6 and 24 h p.i. (Fig. 7A), while *MuPLSCR1like-b* did not show any significant alterations (Fig. 7D). Nonetheless, LPS induction significantly downregulated *MuPLSCR1like-b* after 72 h p.i. (Fig. 7E) without any significant alterations in *MuPLSCR1like-a* expression (Fig. 7B). Moreover, *L. garvieae* treatment did not cause any significant changes in *MuPLSCR1like-a* and *MuPLSCR1like-b* expression (Fig. 7C and F).

4. Discussion

Phospholipid scramblases are the proteins that facilitate rapid movements of phospholipid molecules along bidirectional pathways, ensuring the phospholipid asymmetry in the plasma membrane [10]. The previously identified PLSCR domains have their own distinct functions, which can be clarified separately [3]. From the results obtained in our study on MuPLSCR1like-a and -b, it was possible to identify most of the conserved domains and motifs in their sequences as well as slight differences from other PLSCR1 homologues. Therefore, because they share a common structural topology with PLSCR1 orthologs, MuPLSCR1like-a and -b were categorized as members of the scramblase family. According to a study by Sims et al. [37], human PLSCRs contain multiple PXXP and PPXY domains, which are responsible for the ability of PLSCRs to interact with SH3- and WW domain–containing proteins, except for human PLSCR2. As revealed by our results, the N termini of both MuPLSCR1like-a and -b are not enriched in proline (Pro) residues, thus pointing to their weaker interactions with SH3- and WW domain–containing proteins.

The tertiary structure analysis of MuPLSCR1like-a and -b clearly showed the 12-stranded β-barrel which encompasses the central C-terminal α-helix (Fig. 2), which is a common feature of scramblases [38]. This C-terminal helix has been previously identified as a transmembrane helix that is believed to be hydrophobic [38]. As suggested previously, this hydrophobicity may have developed due to the packing nature of the helix in the core protein domain, and therefore it is not a true transmembrane helix [38]. The 2D graphical representation clearly revealed the membrane-spanning segments of MuPLSCR1like-a and -b. These were formed by antiparallel β-strands, constituting a barrel shape channel that spans the membrane (Fig. 3).

Another major feature of scramblases is a DNA-binding domain, which enables the protein to interact with DNA [3]. As illustrated in Fig. 1, the region 18–51 aa in MuPLSCR1like-a and region 5–37 aa in MuPLSCR1like-b are the DNA-binding motifs, which show low conservation with homologues. Although little evidence is available about the DNA-binding properties of scramblases, studies on human PLSCR1 indicate that it interacts with the inositol 1,4,5-tri-phosphate (IP3) receptor type 1 (*IP3R1*) promoter [39] and is reported to be highly conserved in mice, the fruit fly, zebrafish, and frogs [3]. In human PLSCR1, the DNA-binding motif spans aa residues at positions 86–118 [40]. Its deletion causes misfolding of the β-barrel because of removal of the first β-strand in the domain; there is evidence that this removal eliminates the capacity for DNA binding [38]. Therefore, persistence of DNA-binding motifs in MuPLSCR1like-a and -b probably maintains the correct folding patterns of the β-barrel in their structures, thereby ensuring the DNA-binding ability.

The cysteine palmitoylation motif is another functionally important region that regulates the trafficking of PLSCR to the nucleus or to the plasma membrane [12]. In our study, the cysteine palmitoylation motif was identified only in MuPLSCR1like-a while lacking in MuPLSCR1like-b (Fig. 1.). On the other hand, this motif is conserved in most of the sequences that have been identified previously, except for yeast [3] and planarian (*Dugesia japonica*) sequences [20].

Proteins that are destined to function inside the nucleus contain a classical NLS with three Arg/Lys residues that can form a basic patch over an imported cargo [15]. The classical NLS has been recognized in the SV40 virus (PKKKRLV), which has a positively charged amino acid sequence in its NLS [9]. This sequence is replaced by hydrophobic residues in nonclassical NLS, discovered in human PLSCR1 as the aa sequence ^{257}GKISKHWTGI^{266} [9]. In agreement with that finding, we observed ^{189}GQISKQWGGF^{198} in MuPLSCR1like-a and ^{176}GKISKQWTGL^{184} in MuPLSCR1like-b, suggesting that MuPLSCR1like-a and -b possess a nonclassical NLS (Fig. 1.). The critical lysine residue located at the 5th position of a nonclassical NLS is highly conserved throughout all the examined organisms, and same was obtained in an early study by Sahu et al., in 2007 [3].

A Ca^{2+}-binding EF-handlike domain structure has been identified in human PLSCR1, with two short α-helical segments close to the C terminus, which are separated by 12-residue acidic loops [41]. Nevertheless, the proposed structural model for hPLSCR1 indicates that this motif overlaps with one of the core β-strands of the β-barrel formation around the C-terminal α helix [11]. The same structural features were observed in the predicted 3D structural models of MuPLSCR1like-a and MuPLSCR1like-b in our study (Fig. 2.). Both MuPLSCR1like-a and MuPLSCR1like-b showed highly conserved amino acid residues at positions 1 (D), 3 (D), 5 (F), 7 (I), 9 (F), and 12 (D), which are supposed to contribute to the octahedral loop formation for binding to Ca^{2+} ions, and this arrangement is fully consistent with the predicted EF-handlike motif in hPLSCR1 [3]. According to a hypothesis advanced in early studies, replacement of those selected residues within the motif may abrogate the Ca^{2+}-binding ability of PLSCR1 and the expression of phospholipid scramblase activity too, which depends on the concentration of Ca^{2+} [38]. Therefore, we can suggest that by having conserved amino acid residues at critical positions of the motif, MuPLSCR1like-a and MuPLSCR1like-b may have the same Ca^{2+}-binding affinity as hPLSCR1 does.

Furthermore, the transmembrane domain at the C terminus is essential for scrambling activities [14,42]. Additionally, although the Ca^{2+}-binding domain exists in the sequence, deletion of the C-terminal α-helix of the transmembrane region causes misfolding of the Ca^{2+}-binding site and thereby reduces the Ca^{2+}-binding ability [42]. As depicted in Fig. 1, this transmembrane region is highly conserved among the PLSCR1 homologues including MuPLSCR1like-a and -b. Furthermore, the short tail extending from the C-terminal end to the plasma membrane suggests that MuPLSCR1like-a and MuPLSCR1like-b belong to type II membrane proteins [37].

The constructed phylogenetic tree uncovered the evolutionary relation of MuPLSCR1like-a and MuPLSCR1like-b with other PLSCRs (Fig. 4). All the fish PLSCR1like proteins were clustered in one clade with several other fish PLSCR1 and -2 proteins, thus pointing to their common ancestral origin. Fish from different taxonomic orders and their molecular similarity allowed for formation of subclades within the clade. According to the constructed phylogenetic tree, MuPLSCR1like-a and MuPLSCR1like-b diverged from each other. Because they belong to the same fish species, this divergence may be due to their molecular differences, which we have discussed from the beginning. Nevertheless, in the constructed phylogenetic tree, MuPLSCR1like-a showed a close relation with PLSCR1, just as with the *Danio rerio* protein by separately branching together in the same clade. This phenomenon was also confirmed by 51.6% of shared sequence identity and 63.4% of shared similarity in the pairwise sequence comparison (Table 2). Moreover, MuPLSCR1like-b closely clustered together with *Larimichthys crocea* PLSCR2 with 96.5% sequence identity and 98.7% similarity in their sequences (Table 2). In addition, *Oryzias latipes* PLSCR1 and PLSCR1like proteins from *Seriola dumerili* and *Amphiprion ocellaris* were clustered in the same subclade.

Although PLSCR isoforms are expressed in different locations in the cell, PLSCR1 is present in the plasma membrane [2]. According to the previous studies, hPLSCR1 is expressed in various tissues including the heart, kidneys, pancreas, prostate, and colon whereas hPLSCR2 is expressed in only testis [14]. According to those studies, hPLSCR1 is not detectable in the brain [14,40]. In our study, *MuPLSCR1like-a* and *MuPLSCR1like-b* were detected in all the examined tissues (Fig. 5). Nevertheless, *MuPLSCR1like-a* showed its highest expression in the intestine, while MuPLSCR1like-b was highly expressed in the brain. Although our MuPLSCR1like-a data are consistent with the previous studies on humans, our MuPLSCR1like-b data contradict them: detection in the brain and muscle. This finding suggests that the mRNA expression levels of PLSCRs have species-specific and isoform-specific distribution patterns. The fish intestine is in contact with the external environment through the mouth and gut opening stages and at the onset of feeding, while being exposed to various unfamiliar pathogens.

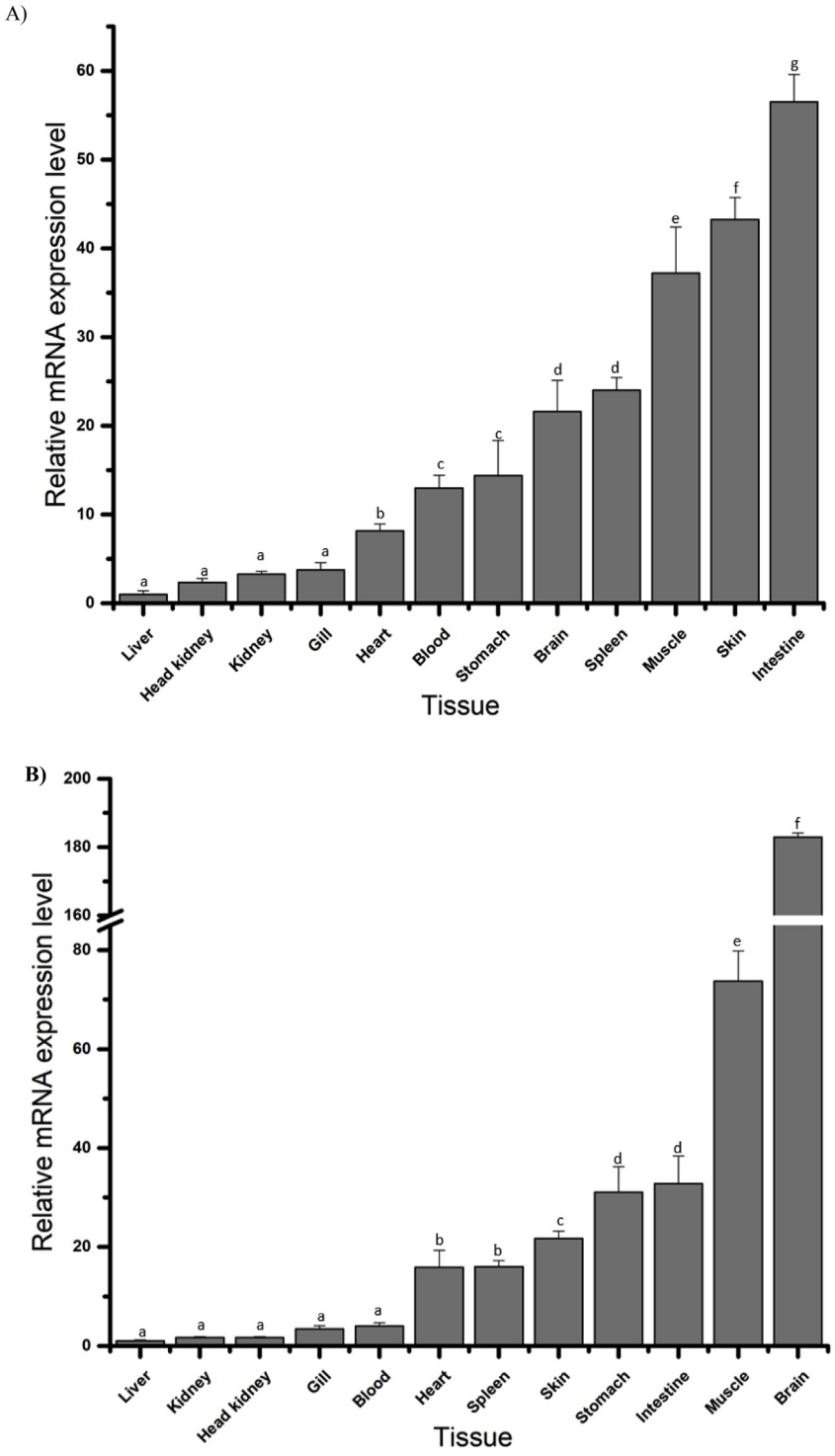

Fig. 5. A) & B) Tissue-specific transcriptional profiles of *MuPLSCR1like-a* & *-b* in red lip mullets. The calculations were performed by the Livak method. Data are presented as mean ± standard deviation (n = 3). Significance of inter-tissue differences was evaluated by one-way analysis of variance (ANOVA) followed by Duncan's multiple-range test in the SPSS 16.0 software. Identical letters indicate the absence of a significant difference ($p < 0.05$) between the tissues.

Therefore, the fish intestine works as a multifunctional organ both performing nutrient uptake and having pathogen recognition mechanisms [43]. According to early studies, mast cells can be activated by PLSCRs, and this event stimulates the secretion of proinflammatory cytokines [21]. During a viral infection, the intestine activates the adipocytokine pathway, which can be induced by proinflammatory cytokines [43]. Therefore, we suppose that the highest amount of MuPLSCR1like-a was present in the intestine for the purpose of protecting the host cells from viral infections. The brain is considered as the main component of the central nervous system (CNS), and microglia are the first responders to CNS injury or diseases [44]. This microglial activation can induce inflammatory responses with the end result of restricting tissue injury or pathogen spread [44]. Due to a viral infection, the CNS activates its innate immune response, which includes microglial phagocytosis [44]. PLSCR1 has been identified as an effective target for the control of microglial phagocytosis, and the greatest

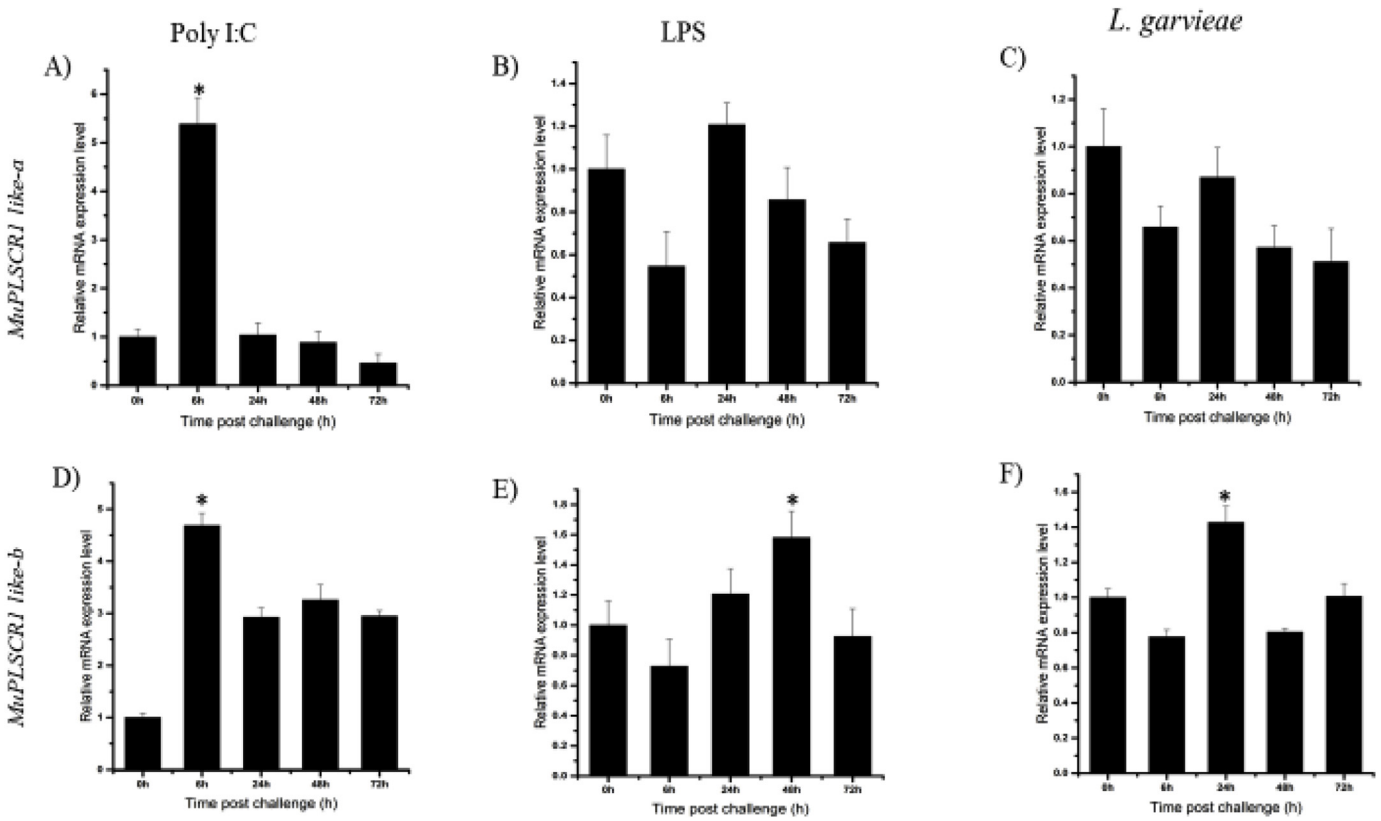

Fig. 6. Relative mRNA expression of *MuPLSCR1like-a* and *MuPLSCR1like-b,* analyzed by qPCR over time in the spleen of red lip mullets (A–F) in response to challenges with poly(I:C) (A, D), LPS (B, E), and *L. garvieae* (C, F). Data are presented as mean ± standard deviation (n = 3). Data marked with a * represent a statistical difference in expression as compared with the 0 h p.i. baseline.

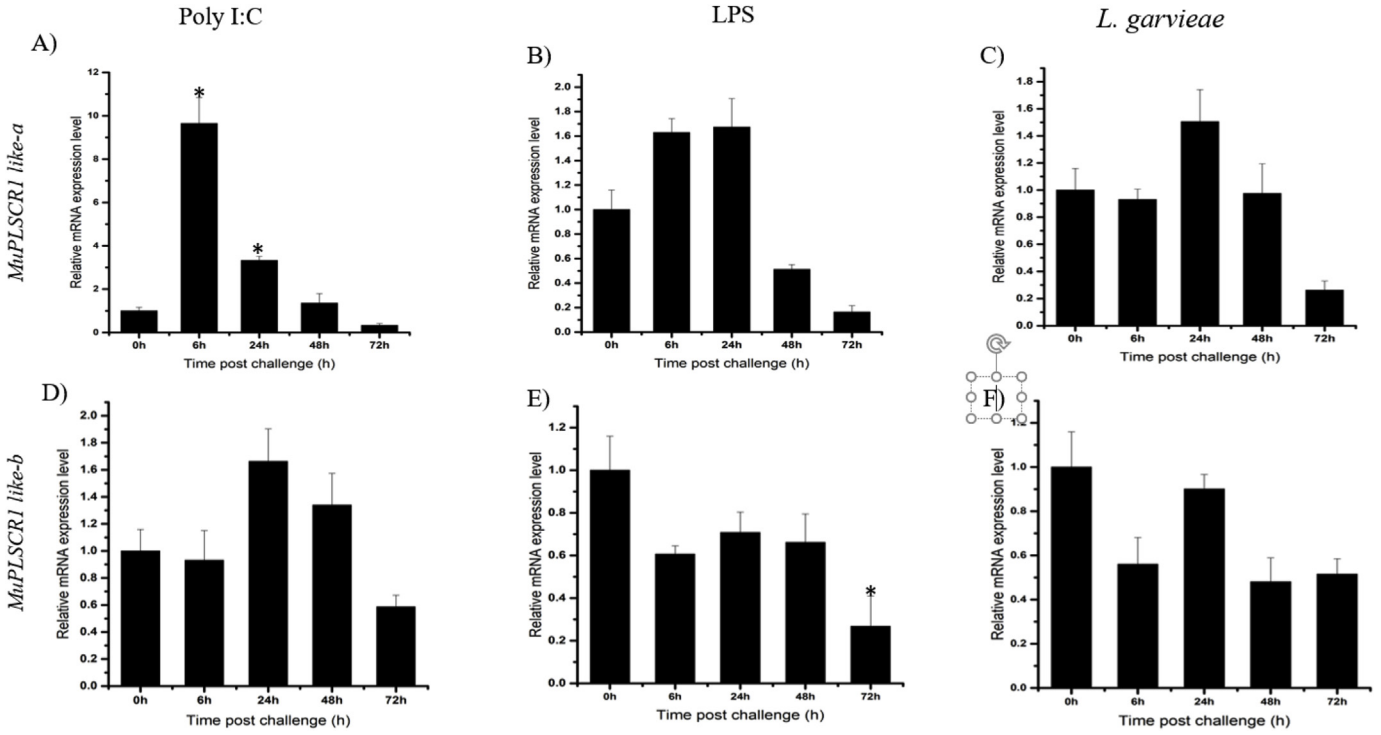

Fig. 7. Relative mRNA expression of *MuPLSCR1like-a* and *MuPLSCR1like-b*, analyzed by qPCR over time in the head kidney of red lip mullets (A–F) in response to challenges with poly(I:C) (A, D), LPS (B, E), or *L. garvieae* (C, F). Data are presented as mean ± standard deviation (n = 3). Data with marked with a * represent a statistical difference in expression as compared with the 0 h p.i. baseline.

expression of MuPLSCR1like-b in the brain as observed in the present study also provides strong evidence for this scenario.

The immune system is present in all the organisms and varies in its complexity including variation in the innate and adaptive components [45]. Fish possess both innate and adaptive immune systems by evolution. At the same time, the fish innate immune system is considered stronger than the adaptive immune system of fish [45]. Immune responses mediated by PLSCRs have been documented in the early studies on mammals [16,17] and planarians [20]. These data prompted us to focus on the immune responses involving *MuPLSCR1like-a* and *MuPLSCR1like-b* in red lip mullets. Out of several immune organs in the fish immune system, the spleen has been identified as a major secondary lymphatic and scavenging organ that has a critical role in hematopoiesis, antigen degradation, and the process of antibody production [45]. Moreover, it performs a major function in trapping of antigens, even though fish do not possess lymph nodes [46]. Furthermore, spleen size of fish is considered a primary indicator of the immune responses to parasitic infections [47]. The head kidney of fish is considered the principal immune organ responsible for phagocytosis, antigen processing, and formation of IgM and immune memory through melanomacrophagic centers [48]. Moreover, the head kidney is an important endocrine organ which possesses major regulatory functions for immune endocrine interactions [48]. Therefore, the spleen and head kidney were used in the present study as the sites for transcriptional analysis to evaluate the immune responses mediated by *MuPLSCR1like-a* and *MuPLSCR1like-b* induced by different immune stimulants.

In the immune challenge experiment, fish were injected with different immune stimulants, including bacteria (*L. garvieae*), a virus mimic (poly[I:C]), and LPS, to determine the responses of *MuPLSCR1like-a* and *MuPLSCR1like-b*. *MuPLSCR1like-a* and *MuPLSCR1like-b* from the spleen and *MuPLSCR1like-a* from the head kidney showed significant upregulation after poly(I:C) treatment, i.e., at 6 h after the injection. Induction with poly(I:C) allows the host cell to express its antiviral functions against pathogens. Viral infections can stimulate IFN-α or -β or IFN-stimulated genes, which can act as major components of an antiviral host defense mechanism [49]. PLSCR1 has been identified as an interferon-stimulated gene (ISG) in previous antiviral studies [16], and many reports are available showing the interferon inducing ability of PLSCRs [13,17,20]. Together with our results, these data led us to suggest that *MuPLSCR1like-a* and *MuPLSCR1like-b* also possess the interferon inducing ability, being related to the PLSCR family, thereby activating the host defense mechanism when infected with viral pathogens. However, in the present study, we observed downregulation of *MuPLSCR1 like a* and *MuPLSCR1 like b,* 6 h after injection of LPS and *L. garvieae*. A previous study on mice macrophages showed FcR-mediated phagocytosis stimulation through the depletion of endogenous PLSCR1, whereas overexpression of PLSCR1 inhibited this process [50]. Among teleost immunoregulatory receptors, leukocyte Iimmune-type receptors (LITRs) have been identified as phylogenetically and structurally related to mammalian FcRs and FcR-like proteins [51]. Moreover, LITR-types associated with the channel catfish (*Ictalurus punctatus*) adaptor proteins IpFcRγ and FcRγ-L have been identified in a previous study, thus revealing the functional significance of this immune receptor-adaptor signaling complex [52]. Therefore, we suggest that the decreasing *MuPLSCR1 like a* and *MuPLSCR1 like b,* 6 h after LPS and *L. garvieae* injection was due to the stimulation of LITRs mediated phagocytosis in red lip mullets.

Moreover, in the spleen, MuPLSCR1*like-b* showed high expression levels in response to LPS and *L. garvieae* treatments. *MuPLSCR1like-a* and *MuPLSCR1like-b* in the head kidney did not show this kind of significant upregulation. One study on *Staphylococcal* α-toxin, a pore-forming toxin from a gram-positive pathogen, has described PLSCR1s' mediation of host cell defense against the critical damage caused by these toxins [17]. Additionally, stimulation with PGN, another component of gram-positive bacteria, significantly upregulates PLSCRs in planarians; thus, PLSCRs help to counteract gram-positive bacterial infections [20]. Furthermore, PLSCR1 upregulation in response to LPS has been observed since early studies on mice [53] and planarians [20].

Nevertheless, the effect of LPS on the PLSCRs is considered isoform-specific and tissue-specific [53]. This arrangement supports the different findings about *MuPLSCR1like-a* and *MuPLSCR1like-b* in our study. Collectively, we suggest that the results obtained in the immune challenge experiment of this study may be explained by the immune response activation via MuPLSCR1like-a and MuPLSCR1like-b as immunity-related proteins.

5. Conclusion

This study provides the first experimental insights into the molecular and transcriptional characteristics of two PLSCR1-related genes in the red lip mullet. In summary, cDNA of two putative PLSCR1-related genes, *MuPLSCR1like-a* and *MuPLSCR1like-b* from the red lip mullet were identified and characterized in the present study. Because of their structural characteristics, phylogenetic relations, and homology analysis, these two genes were confirmed as *PLSCR1*-like genes belonging to the PLSCR family. Transcriptional analysis of *MuPLSCR1like-a* and *MuPLSCR1like-b* revealed their different distribution patterns in different tissues of red lip mullets. The mRNA expression levels of *MuPLSCR1like-a* and *MuPLSCR1like-b* were determined at different time points after the fish were challenged with bacterial or viral components. The significant changes in their expression allow us to propose possible functions of *MuPLSCR1like-a* and *MuPLSCR1like-b* in the innate immune system of red lip mullets.

Acknowledgments

This research was a part of the project titled 'Fish Vaccine Research Center', funded by the Ministry of Oceans and Fisheries, Korea and was supported by a grant from Marine Biotechnology Program (20180430, Genome Analysis of Marine and Fisheries Organisms and Development of Functional Applications) Funded by Ministry of Oceans and Fisheries, Korea.

References

[1] T. Pomorski, A.K. Menon, Lipid flippases and their biological functions, Cell. Mol. Life Sci. 63 (24) (2006) 2908–2921.
[2] F.X. Contreras, L. Sánchez-Magraner, A. Alonso, F.M. Goñi, Transbilayer (flip-flop) lipid motion and lipid scrambling in membranes, FEBS Lett. 584 (9) (2010) 1779–1786.
[3] S.K. Sahu, S.N. Gummadi, N. Manoj, G.K. Aradhyam, Phospholipid scramblases: an overview, Arch. Biochem. Biophys. 462 (1) (2007) 103–114.
[4] P.T. Srinivasan, J. Basu, Altered membrane phospholipid organization and erythrophagocytosis in E beta-thalassemia, Biochim. Biophys. Acta Biomembr. 1285 (1) (1996) 65–70.
[5] B.E.M. Bevers, et al., Is Loss A, (2016), pp. 1983–1991.
[6] P. Williamson, R.A. Schlegel, Transbilayer phospholipid movement and the clearance of apoptotic cells, Biochim. Biophys. Acta Mol. Cell Biol. Lipids 1585 (2–3) (2002) 53–63.
[7] R.F. Zwaal, P. Comfurius, E.M. Bevers, Lipid–protein interactions in blood coagulation, Biochim. Biophys. Acta Rev. Biomembr. 1376 (3) (1998) 433–453.
[8] P. Williamson, E.S. van den, R.A. Schlegel, Phosphatidylserine exposure and phagocytosis of apoptotic cells, Methods Cell Biol. 66 (2001) 339–364.
[9] M.H. Chen, I. Ben-Efraim, G. Mitrousis, N. Walker-Kopp, P.J. Sims, G. Cingolani, Phospholipid scramblase 1 contains a nonclassical nuclear localization signal with unique binding site in importin α, J. Biol. Chem. 280 (11) (2005) 10599–10606.
[10] S. Rayala, V.G. Francis, U. Sivagnanam, S.N. Gummadi, N-terminal proline-rich domain is required for scrambling activity of human phospholipid scramblases, J. Biol. Chem. 289 (19) (2014) 13206–13218.
[11] S.K. Sahu, G.K. Aradhyam, S.N. Gummadi, Calcium binding studies of peptides of human phospholipid scramblases 1 to 4 suggest that scramblases are new class of calcium binding proteins in the cell, Biochim. Biophys. Acta Gen. Subj. 1790 (10) (2009) 1274–1281.
[12] T. Wiedmer, J. Zhao, M. Nanjundan, P.J. Sims, Palmitoylation of phospholipid scramblase 1 controls its distribution between nucleus and plasma membrane, Biochemistry 42 (5) (2003) 1227–1233.
[13] Q. Zhou, et al., Transcriptional control of the human plasma membrane phospholipid scramblase 1 gene is mediated by interferon-alpha, Blood 95 (8) (2000) 2593–2599.
[14] Q. Zhou, J. Zhao, J.G. Stout, R.A. Luhm, T. Wiedmer, P.J. Sims, Molecular cloning

of human plasma membrane phospholipid scramblase, J. Biol. Chem. 272 (29) (1997) 18240–18244.
[15] Y. Huang, et al., Antileukemic roles of human phospholipid scramblase 1 gene, evidence from inducible PLSCR1-expressing leukemic cells, Oncogene 25 (50) (2006) 6618–6627.
[16] B. Dong, et al., Phospholipid scramblase 1 potentiates the antiviral activity of interferon, J. Virol. 78 (17) (2004) 8983–8993.
[17] M. Lizak, T.O. Yarovinsky, Phospholipid scramblase 1 mediates type i interferon-induced protection against staphylococcal beta-toxin, Cell Host Microbe 11 (1) (2012) 70–80.
[18] U. Sivagnanam, S.K. Palanirajan, S.N. Gummadi, The role of human phospholipid scramblases in apoptosis: an overview, Biochim. Biophys. Acta Mol. Cell Res. 1864 (12) (2017) 2261–2271.
[19] K. Segawa, S. Nagata, An apoptotic 'eat me' signal: phosphatidylserine exposure, Trends Cell Biol. 25 (11) (2015) 639–650.
[20] Y. Han, et al., Identification and characterization of a phospholipid scramblase encoded by planarian Dugesia japonica, Gene 602 (2017) 43–49.
[21] U. Acharya, et al., Drosophila melanogaster Scramblases modulate synaptic transmission, J. Cell Biol. 173 (1) (2006) 69–82.
[22] H.J. Han, N.S. Lee, M.S. Kim, S.H. Jung, An outbreak of lactococcus garvieae infection in cage-cultured red lip mullet chelon haematocheilus with green liver syndrome, Fish. Aquat. Sci. 18 (3) (2015) 333–339.
[23] H. Kim, D. Kang, S. Cho, M. Kim, J. Park, K. Kim, Acoustic target strength measurements for biomass estimation of aquaculture fish, redlip mullet (chelon haematocheilus), Appl. Sci. 8 (9) (2018) 1536.
[24] A. Rhoads, K.F. Au, PacBio sequencing and its applications, Genom. Proteom. Bioinf. 13 (5) (2015) 278–289.
[25] S.F. Altschul, W. Gish, W. Miller, E.W. Myers, D.J. Lipman, Basic local alignment search tool, J. Mol. Biol. 215 (3) (1990) 403–410.
[26] T.N. Petersen, S. Brunak, G. von Heijne, H. Nielsen, SignalP 4.0: discriminating signal peptides from transmembrane regions, Nat. Methods 8 (10) (2011) 785–786.
[27] C.J.A. Sigrist, et al., New and continuing developments at PROSITE, Nucleic Acids Res. 41 (D1) (2013) 344–347.
[28] K. Tamura, D. Peterson, N. Peterson, G. Stecher, M. Nei, S. Kumar, MEGA5: molecular evolutionary genetics analysis using maximum likelihood, evolutionary distance, and maximum parsimony methods, Mol. Biol. Evol. 28 (10) (2011) 2731–2739.
[29] H. McWilliam, et al., Analysis tool web services from the EMBL-EBI, Nucleic Acids Res. 41 (Web Server issue) (2013) 597–600.
[30] F. Sievers, et al., Fast, scalable generation of high-quality protein multiple sequence alignments using Clustal Omega, Mol. Syst. Biol. 7 (1) (2014) pp. 539–539.
[31] T. S. Manipulation, Internet On-Ramp Internet On-Ramp, vol. 28, no. 6, 2000.
[32] P.G. Bagos, T.D. Liakopoulos, I.C. Spyropoulos, S.J. Hamodrakas, PRED-TMBB: a web server for predicting the topology of β-barrel outer membrane proteins, Nucleic Acids Res. 32 (WEB SERVER ISS.) (2004) 400–404.
[33] T. Schwede, J. Kopp, N. Guex, M.C. Peitsch, SWISS-MODEL: an automated protein homology-modeling server, Nucleic Acids Res. 31 (13) (2003) 3381–3385.
[34] W. DeLano, Pymol: an open-source molecular graphics tool, CCP4 Newsl. Protein Crystallogr. 700 (2002).
[35] A.F. Page, The MIQE guidelines and assessment of nucleic acids prior to qPCR and RT-qPCR, Therm. Sci. (2010) 1–3.
[36] K.J. Livak, T.D. Schmittgen, Analysis of relative gene expression data using real-time quantitative PCR and the $2-\Delta\Delta CT$ method, Methods 25 (4) (2001) 402–408.
[37] P.J. Sims, T. Wiedmer, Unraveling the mysteries of phospholipid scrambling, Thromb. Haemostasis 86 (1) (2001) 266–275.
[38] A. Bateman, R.D. Finn, P.J. Sims, T. Wiedmer, A. Biegert, J. Söding, Phospholipid scramblases and Tubby-like proteins belong to a new superfamily of membrane tethered transcription factors, Bioinformatics 25 (2) (2009) 159–162.
[39] C.M. Frisby, A matter of life and death, J. Black Stud. 37 (1) (2006) 103–126.
[40] T. Wiedmer, Q. Zhou, D.Y. Kwoh, P.J. Sims, Identification of three new members of the phospholipid scramblase gene family, Biochim. Biophys. Acta Biomembr. 1467 (1) (2000) 244–253.
[41] C. Notredame, D.G. Higgins, J. Heringa, T-coffee: a novel method for fast and accurate multiple sequence alignment, J. Mol. Biol. 302 (1) (2000) 205–217.
[42] L. Sánchez-Magraner, et al., The C-terminal transmembrane domain of human phospholipid scramblase 1 is essential for the protein flip-flop activity and $Ca2+$-binding, J. Membr. Biol. 247 (2) (2014) 155–165.
[43] S.A.M. Martin, C.E. Dehler, E. Król, Transcriptomic responses in the fish intestine, Dev. Comp. Immunol. 64 (2016) 103–117.
[44] Y. Tufail, et al., Phosphatidylserine exposure controls viral innate immune responses by microglia, Neuron 93 (3) (2017) 574–586 e8.
[45] P.R. Rauta, B. Nayak, S. Das, Immune system and immune responses in fish and their role in comparative immunity study: a model for higher organisms, Immunol. Lett. 148 (1) (2012) 23–33.
[46] C.M. Press, B.H. Dannevig, T. Landsverk, Immune and enzyme histochemical phenotypes of lymphoid and nonlymphoid cells within the spleen and head kidney of atlantic salmon (salmo salar l.), Fish Shellfish Immunol. 4 (2) (1994) 79–93.
[47] J. Lovy, J.A. Becker, D.J. Speare, D.W. Wadowska, G.M. Wright, M.D. Powell, Ultrastructural examination of the host cellular response in the gills of Atlantic salmon, Salmo salar, with amoebic gill disease, Vet. Pathol. 44 (5) (2007) 663–671.
[48] L. Tort, J.C. Balasch, S. Mackenzie, Fish immune system. A crossroads between innate and adaptive responses, Immunologia 22 (3) (2003) 277–286.
[49] J. N, et al., Functional role of type I and type 11 interferons in antiviral defense, Science (80-.) 264 (November 1993) (1994).
[50] C. Herate, et al., Phospholipid scramblase 1 modulates FcR-mediated phagocytosis in differentiated macrophages, PLoS One 11 (1) (2016) 1–19.
[51] D.M. Lillico, et al., Teleost leukocyte immune-type receptors activate distinct phagocytic modes for target acquisition and engulfment, J. Leukoc. Biol. 98 (2) (2015) 235–248.
[52] H.D. Cortes, B.C. Montgomery, K. Verheijen, E. García-García, J.L. Stafford, Examination of the stimulatory signaling potential of a channel catfish leukocyte immune-type receptor and associated adaptor, Dev. Comp. Immunol. 36 (1) (2012) 62–73.
[53] B. Lu, et al., Expression of the phospholipid scramblase (PLSCR) gene family during the acute phase response, Biochim. Biophys. Acta Mol. Cell Biol. Lipids 1771 (9) (2007) 1177–1185.